LATITUDINAL DISTRIBUTION OF CO_2 ICE ON ARIEL CONSISTENT WITH SEASONAL MIGRATION.

R. J. Cartwright[1], T. A. Nordheim[2], W. M. Grundy[3,4], D. DeColibus[5], M. M. Sori[6], C. B. Beddingfield[1,7], E. J. Leonard[2], C. M. Elder[2], C. J. Cochrane[2], L. H. Regoli[8], D. H. Atkinson[2], B. J. Holler[9], D. P. Cruikshank[6], J. P. Emery[4]. [1]The SETI Institute, Mountain View, CA, [2]Jet Propulsion Laboratory, Pasadena, CA, [3]Lowell Observatory, Flagstaff, AZ, [4]Northern Arizona University, Flagstaff, AZ, [5]New Mexico State University, Las Cruces, NM, [6]Purdue University, West Lafayette, IN, [7]NASA Ames Research Center, Mountain View, CA, [8]John Hopkins University Applied Physics Laboratory, Laurel, MD, [9]Space Telescope Science Institute, Baltimore, MD, (rcartwright@seti.org).

Introduction: Ground-based, near-infrared (NIR) observations of the classical Uranian moon Ariel have determined that its surface composition is primarily composed of H_2O ice mixed with dark and spectrally neutral constituents that likely include a carbon-rich component (e.g., [1-3]). CO_2 ice also has been detected on Ariel via three prominent absorption features centered near 1.966, 2.012, and 2.070 μm, which are stronger on Ariel's trailing hemisphere (longitudes 181 – 360º) compared to its leading hemisphere (longitudes 1 – 180º) [4-6]. The spectral signature of these three CO_2 bands is remarkably consistent with "pure" CO_2 ice measured in the laboratory (i.e., segregated from other constituents in concentrated deposits with crystal structures dominated by CO_2 molecules) (e.g., [7,8]). It has been hypothesized that CO_2 ice on Ariel, and the other classical Uranian moons, is formed by ongoing charged particle bombardment of native H_2O ice and C-rich material on their surfaces [4-6]. Alternatively, CO_2 ice could be a native constituent that is sourced from the interiors of the Uranian satellites.

At the estimated peak surface temperatures of the Uranian moons (80 – 90 K, [9-10]), Regolith-mixed CO_2 ice is thermodynamically unstable over geologic timescales [5,10]. Because of the large obliquity of the Uranian system (~98º), the poles of the Uranian moons are bathed in continual sunlight during their respective long summer seasons. As a result, long term cold traps for CO_2 ice are likely concentrated at low latitudes on these moons, where peak temperatures are experienced for shorter periods of time compared to their poles [5,10]. Consequently, CO_2 molecules generated or exposed at polar latitudes should sublimate, migrate to low latitudes, and condense in cold traps.

Previously analyzed NIR spectra of Ariel were collected during late southern summer and northern spring (subsolar latitudes 30ºS – 25ºN), when low latitude regions that could be rich in CO_2 were near the center of Ariel's observed disk. Here, we present updated results on the distribution of CO_2 ice on Ariel using new spectra collected during late northern spring, when the center of Ariel's observed disk was over mid (30 – 45ºN) and high (45º – 51ºN) latitudes.

Data and Observations: We collected ten NIR reflectance spectra using the SpeX spectrograph [11] on NASA's Infrared Telescope Facility (IRTF), between 2014 and 2020 and five reflectance spectra with the TripleSpec spectrograph [12] on the 3.5-m telescope at Apache Point Observatory (APO) in 2019 and 2020 (example spectra shown in Figure 1). Data extraction, wavelength calibration, standard star division, co-adding of exposures, and spectral order merging was conducted using the Spextool Data Reduction suite [13] and custom programs. Some spectra were divided by a scaled atmospheric transmission spectrum to correct for residual telluric CO_2 bands between 1.9 and 2.1 μm (reduction steps described in more detail in [6]).

Band Parameter Measurements: All 15 reduced spectra were analyzed using an existing band parameter analysis program. To measure the three prominent CO_2 ice features centered near 1.966, 2.012, and 2.070 μm (hereafter referred to as CO_2 bands 1, 2, and 3, respectively), we first divided each feature by its continuum and then used the trapezoidal rule to calculate the area of the resulting continuum-divided band. Band area uncertainties were estimated using Monte Carlo simulations, resampling the 1σ errors for the spectral channels in each band. Next, we summed the three CO_2 band areas into a final integrated band area for each spectrum and propagated errors (band parameter analysis described in more detail in [6]).

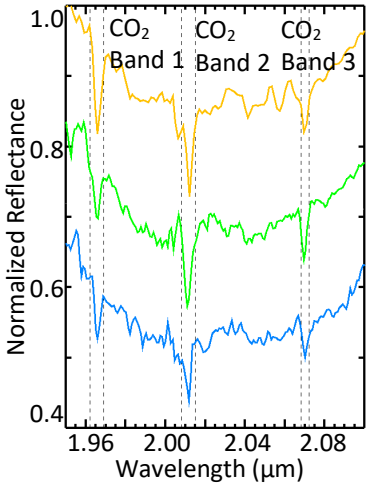

***Figure 1**: CO_2 ice bands 1, 2, and 3 detected in spectra of Ariel (dashed lines), collected near sub-observer longitude 295°. These spectra were collected in three different latitude zones: low, 30°S – 30°N (yellow); mid, 30°N – 45°N (green); and high, > 45°N (blue).*

Results and Analyses: The CO_2 integrated band areas display clear evidence for reduced CO_2 band strengths between spectra collected at similar longitudes (within ± 5°) but in different latitudinal zones: low, 30°S – 30°N; mid, 30°N – 45°N; and high, > 45°N (Figure 2).

To further investigate these latitudinal disparities, we calculated the mean integrated band areas for each of the three latitudinal zones (Figure 3). These mean measurements show a subtle decease in CO_2 integrated band areas on Ariel's trailing hemisphere in the high latitude zone compared to the mid and low latitude zones (> 1σ). We also calculated the mean band area for CO_2 bands 1, 2, and 3 for each latitudinal zone on Ariel's trailing hemisphere (Figure 4). These measurements show similar band strengths for CO_2 band 1 in all three latitudinal zones (< 1σ difference), whereas CO_2 bands 2 and 3 show a significant change in band strength (> 2σ difference). Mean CO_2 band measurements made using the spectra collected over Ariel's leading hemisphere do not display any trends in their latitudinal distributions (< 1σ difference). In general, spectra collected in the mid latitude zone have mean CO_2 band areas that are more similar to spectra collected in the low latitude zone compared to the high latitude zone.

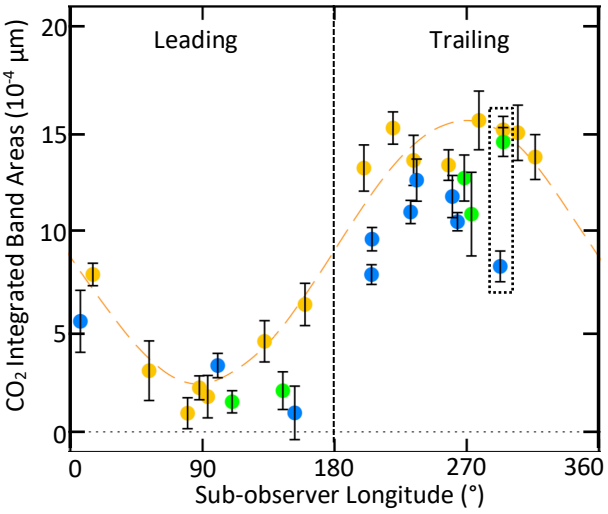

Figure 2: *CO_2 ice integrated band areas and 1σ uncertainties for Ariel, plotted as a function of sub-observer longitude and color-coded by latitude zone: low (yellow), mid (green), and high (blue). Sinusoidal fit to the low latitude zone (yellow dashed line) highlights Ariel's strong leading/trailing asymmetry in CO_2 ice. CO_2 band area measurements for the three spectra shown in Figure 1 are highlighted (dotted box).*

Conclusions and Future Work: The measurements reported here indicate that CO_2 ice bands are weaker at high latitudes on Ariel compared to low latitudes, in particular for CO_2 bands 2 and 3. The reduction in CO_2 band strengths at high latitudes supports the hypothesis that the abundance of CO_2 ice is lower at Ariel's poles and that long term CO_2 cold traps are at low latitudes. Radiative transfer modeling of CO_2 ice bands detected in the high latitude spectra of Ariel, and comparison to spectral models made using low latitude spectra [6], will provide additional insight into the latitudinal distribution of CO_2 ice on Ariel. Continued observations of Ariel over the next decade, as the Uranian system progresses into northern summer (solstice in 2028), will provide key data for volatile transport models, thereby improving our understanding of how CO_2 migrates in response to subsolar heating.

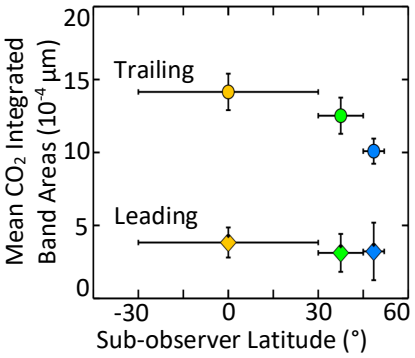

Figure 3: *Mean CO_2 ice integrated band areas and 1σ uncertainties (vertical error bars) for Ariel's leading (diamonds) and trailing (circles) hemisphere, color-coded by latitude zone: low (yellow), mid (green), and high (blue).*

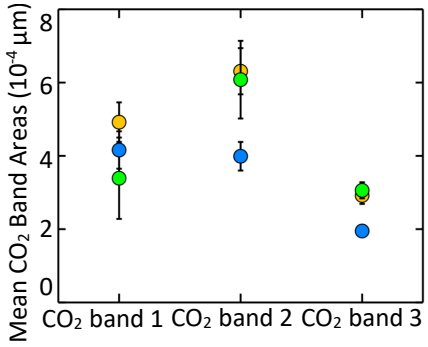

Figure 4*: Mean band areas and 1σ uncertainties for CO_2 bands 1, 2, and 3 (centered near 1.966, 2.012, and 2.070 µm, respectively), color-coded by latitude zone: low (yellow), mid (green), and high (blue).*

References: [1] Cruikshank D. P. et al. (1977) *A&J*, 217, 1006. [2] Brown R. H. and Cruikshank D. P. (1983). *Icarus* 55, 83. [3] Brown R. H. and Clark R. N. (1984). *Icarus* 58, 288. [4] Grundy W. M. et al. (2003) *Icarus*, 162, 222. [5] Grundy W. M. et al. (2006) *Icarus*, 184, 543. [6] Cartwright R. J. et al. (2015) *Icarus*, 257, 428. [7] Hansen G. B. (1997) *Adv. Space Res.* 20, 1613. [8] Gerakines P. A. et al. (2005) *A&J*, 620, 1140. [9] Hanel R. et al. (1986) *Sci.* 233, 70. [10] Sori M. M. et al. (2017) *Icarus*, 290, 1. [11] Rayner J. T. et al. (2003) *Astro. Soc. Pac.* 115, 362. [12] Wilson J. C. et al. (2004) *Ground-based Instrumentation Astro.* 5492, 1295. [13] Cushing M. C. et al. (2004) *Astro. Soc. Pac.* 116, 362.